

*Author Version of : Aquatic Sciences, vol.80(4); 2018; Article no: 38,*

**Significance of metabolically active bacterioplankton in the frontal regions of the  
Northeastern Arabian Sea**

**Lidita Khandeparker\*, Ranjith Eswaran, Niyati Hede, Anil, A.C.**  
CSIR-National Institute of Oceanography, Dona Paula, Goa-403004, India:

Formatted: Font: Not Bold, Italic

Formatted: Font: Italic

Formatted: Left: 0.75", Right: 0.75", Header distance from edge: 0.5", Footer distance from edge: 0.5"

Formatted: Font: Not Bold, Italic

Formatted: Font: 12 pt, Not Bold, Italic, Complex Script Font: 12 pt

Formatted: Font: 13 pt, Complex Script Font: 13 pt

Formatted: Centered

Formatted: Centered, Space After: 0 pt, Line spacing: single

Formatted: Font: Not Bold

Formatted: Line spacing: single

\*Corresponding author. Tel.: +91(0)832-2450432; fax: +91(0)832-2450615.  
Email: [klidita@nio.org](mailto:klidita@nio.org)

Formatted: Normal, Centered, Line spacing: single

Formatted: Centered

**Significance of metabolically active bacterioplankton in the frontal regions of the  
Northeastern Arabian Sea**

Formatted: Space After: 6 pt, Line spacing: single

**Lidita Khandeparker\*, Ranjith Eswaran, Niyati Hede, Anil, A.C.**

~~CSIR-National Institute of Oceanography, Dona Paula, Goa-403004, India.~~

#### **Abstract**

The Northeastern Arabian Sea (NEAS) experiences convective mixing during winter monsoon, which facilitates nutrient enrichment in the surface layers. This region is also known to harbour several sea surface temperature (SST) fronts and filaments, hotspots of primary production and bacterioplankton activity, which play an important role in the microbial loop. Observations on bacterioplankton with an emphasis on their physiological state, i.e., metabolically active (HNA; High Nucleic Acid content) bacteria and metabolically inactive (LNA; Low Nucleic Acid content) bacteria were carried out in the NEAS region during early and peak winter monsoon (EWM and PWM). HNA bacteria were dominant in frontal zones coupled with high bacterial production (BP) indicating their significant role, whereas, LNA bacteria were abundant in non-frontal regions irrespective of the seasons. The differentiation in bacterial metabolic types points out organic matter enrichment in the fronts. During PWM, the nutrient concentration increased resulting in a further increase in HNA bacteria and BP in frontal regions. The transparent exopolysaccharides (TEP) were also higher in frontal zones, and inversely related to total bacterial abundance indicating a fast turnover of the organic matter. The age of the front and background condition prior to the formation of the front influences the relative contribution by bacterioplankton food web dynamics and these attributes would probably also help predict bacterial activities.

**Keywords:** Bacteria; Northeastern Arabian Sea (NEAS); Fronts; Transparent exopolysaccharides (TEP); Protists; Temperature.

## Introduction

The Arabian Sea possesses many qualities that make it unique among the world's oceans. It is highly productive and a distinctive tropical basin characterised by intense meteorological forcing during the summer monsoon (Madhupratap et al. 1996; Shankar et al. 2005). The northeastern Arabian Sea (NEAS) also experiences high production during the winter monsoon due to a convective mixing process bringing nutrients to the surface from the base of the mixed layer (Banse and McClain 1986; Madhupratap et al. 1996). This region is also known to harbour several SST fronts and filaments during this time (Solanki et al. 2008; Roy et al. 2015; Vipin et al. 2015). Fronts and filaments are regions of enhanced biological activity with a greater accessibility of nutrients in contrast to adjacent waters (Fernández et al. 1994; Videau et al. 1994; Read et al. 2000; Muelbert et al. 2008; Belkin et al. 2009; Samo et al. 2012; Lohmann and Belkin, 2014). A recent study in California current ecosystem (CCE) described the role of dynamic microbial populations in carbon cycling at oceanic fronts and this study shed light on the role of hydrography in regulating the metabolism and growth of autotrophic and heterotrophic microbes (Samo et al. 2012 and references within). In such hot spots of primary production, one can expect an enhancement in the dissolved organic matter (DOM). The DOM is mainly composed of sticky, acidic polysaccharides, which further aggregate into transparent exopolysaccharides (TEP) (Schuster and Herndl 1995; Grossart and Simon 1997; Søndergaard et al. 2000). Bacteria are often found embedded within or attached to TEP particles (Passow and Alldredge 1994; Grossart et al. 2006). Moreover, these particles and their precursors are utilized as organic substrates by heterotrophic organisms (Passow 2002). The Biological Carbon Pump (BCP) transfers these organic rich particles from the sunlit surface waters to the ocean's interior (Sanders et al. 2014), and this fuels heterotrophic microbial population (bacteria and protists) via the microbial loop (Azam et al. 1983). Earlier studies have reported maximal bacterial biomass and growth rates in the frontal regions of North Atlantic as well as Mediterranean waters (Pedrós-Alió et al. 1999; Tarran et al. 2001). However, the response of microbial communities varies with the environmental conditions, thus featuring their importance in different biological processes (Samo et al. 2012).

The present study was undertaken in the Northeastern Arabian Sea, which has a wide continental shelf. This region is also known for active fishing and is facilitated by upwelling during summer monsoon and convective mixing during the winter monsoon. Earlier observations in this region under a large interdisciplinary program 'Ocean Finder' had characterized physical signatures and diversity of phytoplankton through chemotaxonomy (Vipin et al. 2015; Roy and Anil 2015). It is pertinent to note that bacterial dynamics forms an integral part of such productive systems. Studies in

temperate frontal regions reveal a significant increase in bacterial abundance, biomass and production within the frontal regions as compared to outside/surrounding water column (Landry et al. 2012; Samo et al. 2012; Taylor et al. 2012). However, no such study has been conducted in the tropical region. The temperature fronts represent diverse hydrographic conditions (high nutrients, low water temperature), heterotrophic bacteria seem to play an important role in the frontal regions with congregated biomass and turnover of organic matter.

Although several studies have examined heterotrophic bacterial dynamics in the Arabian Sea (Ducklow 1993; Ramaiah et al. 1996; 2000; Wiebinga et al. 1997; Pomeroy and Joint 1999), no studies are conducted on their response and role in the frontal regions. We hypothesised that depending on the physical environment the response of heterotrophic bacteria would be different, especially the higher biomass and activity are asserted to occur in fronts and filaments when compared with non-frontal regions. In view of this, the following objectives were laid (i) To investigate the physiological state of microbes in the temperature fronts in the NEAS during early and peak winter monsoon and (ii) To evaluate their role in the dynamic frontal food web systems.

## Materials and Methods

### Description of the study site and sampling

The present study is part of Ocean Finder program. Two cruises were undertaken under this program in the eastern Arabian Sea. The first cruise was from 23<sup>rd</sup> November to 11<sup>th</sup> December 2012 corresponding to early winter monsoon (EWM). The second cruise was conducted in the peak winter monsoon (PWM) from 22<sup>nd</sup> January to 3<sup>rd</sup> February 2014. The study area is located off Gujarat coast of the Northeastern Arabian Sea (Fig. 1). The physical signatures such as temperature and salinity results during EWM cruise revealed that the front and filament sections were distinct from the surrounding waters (Vipin et al. 2015). Similar signatures with enhanced nutrient concentrations were evident during PWM cruise (Roy and Anil 2015; Sarma et al. 2015). The front and filament sections in NEAS were dominated by nanoplanktonic Prymnesiophytes and Prasinophytes, and non-frontal section showed the dominance of picoplankton (*Prochlorococcus*). A total of 26 stations were sampled during EWM and PWM cruises in NEAS region. Seawater samples were collected using 10 l Niskin bottles fitted to the rosette frame (Model: ODF; SBE32) with Sea-Bird Electronics (SBE) 9plus Conductivity-Temperature-Depth (CTD) probe (ODF #381) consisting of a dual temperature (SBE3plus), dual conductivity (SBE4) sensor, dissolved oxygen (SBE43),

Formatted: Indent: First line: 0.32", Space After: 6 pt, Line spacing: 1.5 lines

Formatted: Space After: 6 pt, Line spacing: 1.5 lines

transmissometer (Wetlabs C-Star) and fluorometer (Sea point Sensors). During the EWM cruise, 20 CTD stations were sampled for the total bacterial count (TBC), high nucleic acid and low nucleic acid content (HNA and LNA) bacteria, TEP, protists, and nutrients between (69.2 °E, 18.85 °N) to (69.2 °E, 20.50 °N) as depicted in Fig. 1. During the PWM cruise, 6 CTD stations were sampled for similar parameters in the same region, (Fig. 1) that includes 2 frontal (T1-F and T2-F) and 4 non-frontal stations (T1-NF and T2-NF) from two transects between 69.34 °E, 19.67 °N - 68.74 °E, 20. 24 °N.

The methods followed for nutrient analysis (mainly nitrite, nitrate, silicate, and phosphate) and chl *a* are provided in Roy et al. (2015).

#### **Enumeration of Total Bacterial Count (TBC) and protists**

Aliquots of 4.5ml were taken in triplicates from each CTD cast for TBC and protists analysis and fixed with 1% paraformaldehyde final concentration and stored at -80 °C until samples could be processed on shore (not more than a month). The samples were thawed at room temperature and subsequently stained with SYBR Green I (1:10000 final concentration Molecular Probes, USA) and incubated in the dark for 15 mins before measurement. Flow cytometric absolute cell counting was achieved using BD FACS Aria II instrument equipped with a 488nm blue laser using 1µm size fluorescent beads (Polysciences, USA) as an internal standard. The sheath fluid was BD FACS flow. Emitted light was collected through the following filter sets: (1) 488/10 band pass for right angle light scatter (RALS/SSC) and (2) 530/30 band pass for green fluorescence. The total bacterial abundance (TBC) was expressed as cells L<sup>-1</sup>. High Nucleic Acid content (HNA) bacteria were discriminated from Low Nucleic Acid content (LNA) bacteria. Each subgroup was defined by gating against right angle light scatter (RALS) versus the green fluorescence (FITC). The flow cytometric data were processed using BD FACS Diva (version 6.2) software (Khandeparker et al. 2017).

For protists enumeration, the photomultiplier tube (Detector) was standardised by reducing the voltage with reference to SSC vs green fluorescence so that bacteria would be below the detection threshold as described by Christaki et al. (2011). Emitted light was collected through the following filter sets: (1) 488/10 band pass for right angle light scatter (SSC), (2) 530/30 band pass for green fluorescence and (3) 695/40 for red fluorescence. Further, the bacteria and protists abundance was integrated over the depth by adding the areas of rectangles with the base equal to the difference in depth between two sample points and length equal to the abundance of the deepest sampled depth

Formatted: Indent: First line: 0.32", Space After: 6 pt, Line spacing: 1.5 lines

Formatted: Space After: 6 pt, Line spacing: 1.5 lines

(Chin-Leo and Benner 1992).

### **Bacterial production (BP)**

In the present study, 5-Bromo-2-Deoxyuridine (BrdU) was used for bacterial production (BP) in the NEAS samples which were collected during PWM cruise. Various studies have successfully applied BrdU in measuring the metabolically active cells and bacterial production (BP) in aquatic environments (Hamasaki et al. 2004; Nelson and Carlson 2005; Pernthaler et al. 2002; Steward and Azam 1999). BrdU is an analog of thymidine and binds to actively synthesizing DNA in place of thymidine. BrdU was added to the water samples (1 $\mu$ M final concentration; BD-Biosciences, USA) and incubated for 3 hrs in the dark at in situ temperature. After incubation, the samples were fixed with 0.22  $\mu$ m filtered paraformaldehyde (1 % final concentration) and stored at -80 °C until BrdU immunofluorescence detection. Immunofluorescence staining was performed using FITC labelled anti-BrdU with DNase (BD-Biosciences, USA). BrdU fixed samples were thawed to room temperature and stained with FITC labelled anti - BrdU with DNase (BD-Biosciences, USA as per manufacturer's instructions) for 30 min in dark and analyzed using a BD FACSAria™ II flow cytometer equipped with a 488nm nuclear blue laser. Control samples were also prepared without the addition of anti-BrdU. Emitted light and fluorescence signals were collected through different filter sets: (1) 488/10 band pass for right angle light scatter (RALS), (2) 530/30 band pass filter for green fluorescence signal from anti-BrdU (Eswaran and Khandeparker 2017). Further bacterial carbon production was calculated using 11 fg C per bacterium as a cell-to-carbon conversion factor and expressed as  $\mu$ g C l<sup>-1</sup> h<sup>-1</sup> (Garrison et al. 2009).

### **Transparent exopolysaccharides (TEP) estimation**

TEP were estimated by using the colorimetric method described by Klein et al. (2011). Briefly, 100 ml of seawater was filtered in triplicate onto a 0.4  $\mu$ m polycarbonate filter (Millipore). After filtration, particulate material present on the filter paper was immediately resuspended in 5ml of GF/F filtered seawater and centrifuged for 10 min at 3200  $\times$  g. After centrifugation pellets were stored at -20°C until analysis. During the analysis, the pellets were treated with 2 ml of 0.02% Alcian Blue prepared in 0.06% acetic acid. Subsequently, the samples were centrifuged (3200  $\times$  g, 20 min) to remove the excess dye. The pellets were then rinsed several times with 1 ml of distilled water and centrifuged until a clear supernatant was obtained. A volume of 4 ml of 80% H<sub>2</sub>SO<sub>4</sub> was then added to the pellets. After 2hrs, the absorption of the supernatant was measured by

spectrophotometer at 787 nm. TEP values are expressed as xanthan gum weight equivalent ( $\mu\text{g}$  equiv.  $\text{X l}^{-1}$ ), calculated by using xanthan gum standard calibration curve. Depth integrated concentration was calculated as described above.

### Statistical analysis

The data were log transformed to meet the normality assumption. Before data analysis, log-transformed data were tested for normality using Shapiro-Wilk's W test using STATISTICA 8.0 software. The datasets fulfilling the assumptions for parametric analysis were analysed through one-way analysis of variance (ANOVA), for evaluating significant variations between the frontal and non-frontal regions, followed by post hoc Tukey's HSD test (Bonferroni corrected). Further, a correlation matrix (STATISTICA 8.0) was used to determine the relationship among the biotic (bacterial abundance, HNA, LNA, protists TEP, and Chl *a*) and abiotic (temperature, salinity, nitrate, nitrite, phosphate, silicate) parameters wherein Bonferroni correction was also applied to avoid false positive results at the significance level of  $\leq 0.01$ .

## Results

### Environmental variables

During EWM, a warm parcel of water was encountered on the southern side of transect between 18.85 - 19.25 °N from station 1 to 9 (Fig. 2a-b). However, towards the north the CTD data showed two relatively cold parcels of water between 19.25 - 19.48 °N and 19.95 - 20.20 °N with a temperature decrease of 0.5 to 1.0 °C. Based on their physical characteristics, the first feature was identified as a filament between stations 10 to 14 and the second one as a front from stations 19 and 20 (Fig. 2a-b). Similar to temperature, salinity was also low and ranged from 35.7- 36.55 PSU at the surface in the filament and front region. In the case of PWM, the sea surface temperature (SST) in the frontal regions were 0.56 – 1.02 °C lower than the surrounding water column (Fig. 3a-b). The salinity variations between fronts and non-fronts ranged from 0.03 to 0.13 PSU (Fig. 3b). Similarly, Chl *a*, which is an indicator of phytoplankton biomass also increased from south to the northern frontal region ( $df = 2$ ;  $F = 13.73$ ;  $p = 0.000$ ) (Fig. 3b). The dissolved nutrient concentrations revealed low nitrate levels at subsurface layers of frontal areas and higher below the mixed layer depth (MLD). A similar trend was also observed for phosphate.

Formatted: Space After: 6 pt, Line spacing: 1.5 lines, Don't adjust space between Latin and Asian text, Don't adjust space between Asian text and numbers

Formatted: Space After: 6 pt, Line spacing: 1.5 lines

### Early Winter Monsoon cruise (EWM)

The TBC in the warm patch, filament, and frontal waters ranged between  $1.63 \times 10^7$  and  $1.85 \times 10^9$  cells  $L^{-1}$  (Fig. 4a), was higher in the filament ( $3.64 \times 10^8$  cells  $L^{-1}$ ) and the front ( $3.33 \times 10^8$  cells  $L^{-1}$ ) and low in the warm patch region ( $2.47 \times 10^8$  cells  $L^{-1}$ ) (Fig. 4a). High TBC in the filament and the front was negatively related to TEP (Table. 1a). The depth-integrated bacterial abundance was calculated as described above. The integrated bacterial abundance was significantly higher at station 9, which is located close the filament when compared to other stations (Fig. 5a). Similar to TBC, the HNA bacterial abundance was also high in the front ( $8.96 \times 10^7$  cells  $L^{-1}$ ) and the filament ( $7.30 \times 10^7$  cells  $L^{-1}$ ) and decreased in the warm patch region ( $6.81 \times 10^7$  cells  $L^{-1}$ ) (Fig. 4b). The one-way ANOVA also indicated that the HNA bacterial abundance significantly varied from south to north frontal region ( $df = 2$ ;  $F = 3.245$ ;  $p = 0.04$ ), and their high abundance was positively related to TBC and chl *a* indicating that most of the population in the fronts and filaments were metabolically active when compared with the warm patch (Table. 1a). HNA bacteria also showed a significant negative relation to dissolved nutrients (Table. 1b). Whereas, LNA bacteria were higher in the warm patch ( $7.56 \times 10^7$  cells  $L^{-1}$ ) and least in the frontal region ( $6.77 \times 10^7$  cells  $L^{-1}$ ) (Fig. 4c).

Protist abundance in the warm patch, filament, and frontal waters was typically  $10^7$  cells  $L^{-1}$ . It varied between  $5.93 \times 10^6$  and  $8.53 \times 10^7$  cells  $L^{-1}$  (Fig. 4d). The abundance was higher in the front ( $2.33 \times 10^7$  cells  $L^{-1}$ ) when compared with the filament ( $1.63 \times 10^7$  cells  $L^{-1}$ ) and positively related to HNA bacterial abundance (Table.1a). The depth-integrated protist abundance was also higher in the frontal region (Fig. 5b). The ratio between bacteria and protist was higher in the MLD of the filament and frontal regions indicating a high abundance of heterotrophic bacteria in these regions (Fig. 4e).

TEP ranged from 84 – 1086  $\mu g$  equiv.  $X L^{-1}$  along the transect (Fig. 4f). The concentration was higher in the surface waters of the filament. However, below MLD and in the mixed layer waters of warm patch region patches of TEP were evident, where depth-integrated values for protists and HNA bacteria were lower (Fig. 5c). Besides, depth-integrated TEP concentration did not show variation from warm patch to the frontal section, except at station 1 at the southern side of the warm patch. Interestingly, TEP and HNA signatures were also seen towards the edge of the filament at 19.55 °N at high concentration at the surface; the depth of MLD was very shallow (~20 m). A significant inverse relation was observed between depth-integrated TBC and TEP in the filament ( $r = -0.98$ ,  $p = 0.002$ ).

### Peak Winter Monsoon (PWM)

In the case of PWM, the TBC, HNA bacteria, and TEP values were higher when compared with EWM. During PWM, TBC abundance in the frontal and non-frontal regions was significantly different ( $df = 1$ ;  $F = 8.36$ ;  $p = 0.006$ ) and ranged between  $4.35 \times 10^8 - 6.65 \times 10^9$  cells  $L^{-1}$  (Fig. 6a). Similarly, HNA and LNA bacteria were also twice as high during PWM wherein frontal stations were dominated by HNA bacteria ( $df = 1$ ;  $F = 10.66$ ;  $p = 0.02$ ) and adjacent non-frontal stations by LNA bacteria (Fig. 6c, e). Further, high HNA abundance in the frontal region was positively correlated with Chl *a* ( $r = 0.43$ ;  $p = 0.006$ ;  $n = 16$ ). The values for the depth-integrated TBC, HNA and LNA bacteria were one fold higher during PWM as compared to EWM (Fig. 5a, 7a).

BP was significantly higher in the frontal regions especially in the T2-F front ( $df = 1$ ;  $F = 43.55$ ;  $p = 0.000$ ) (Fig. 6b). Further, BP showed a strong positive correlation with HNA bacteria ( $r = 0.49$ ;  $p = 0.01$ ;  $n = 16$ ). Overall, BP ranged between  $0.09 - 10.04 \mu g C l^{-1} h^{-1}$  in the non-frontal and  $1.45 - 21.54 \mu g C l^{-1} h^{-1}$  in the frontal stations respectively. The production rate was ~2 to 4 fold higher in the fronts as compared to non-fronts (Fig. 6b).

The variations in the protist abundance with reference to fronts differed between the seasons. Their abundance ranged from  $10^6 - 10^8$  cells  $L^{-1}$  (Fig. 6d) and was high during PWM. It varied between  $9.11 \times 10^6 - 1.03 \times 10^8$  cells  $L^{-1}$  and was higher in the non-frontal region. The depth-integrated values were high during EWM. During PWM, protists were high outside the frontal regions and among the fronts were more abundant near the front, T2-F (Fig. 7b).

TEP ranged from 314 - 1212  $\mu g$  equiv.  $X L^{-1}$  and were twice as high during PWM (Fig. 6g). Low levels of TEP in the T1-F frontal stations were consistent with the elevated BP and HNA (Fig. 6b, c, and g). The depth-integrated TEP values were higher during PWM at T2-F (Fig. 7c).

### Discussion

In the present study area, i.e. NEAS, the bacterial populations were categorized into HNA and LNA bacteria. The occurrence of HNA and LNA bacteria in different water masses and seasons could be related to nutrient availability. Overall, the nutrients were high at the surface in the frontal regions during both the seasons. Moreover, during the PWM, an increase in nitrate, phosphate, and silicate at the surface was evident as compared to EWM (Roy and Anil 2015). The metabolically active HNA

Formatted: Indent: First line: 0.32", Space After: 6 pt, Line spacing: 1.5 lines

Formatted: Space After: 6 pt, Line spacing: 1.5 lines

Formatted: Indent: First line: 0.32", Space After: 6 pt, Line spacing: 1.5 lines, No widow/orphan control, Don't allow hanging punctuation, Adjust space between Latin and Asian text, Adjust space between Asian text and numbers

Formatted: Space After: 6 pt, Line spacing: 1.5 lines

bacteria were dominant in the frontal regions when compared with the non - frontal regions irrespective of the seasons. In the aquatic environments, heterotrophic bacteria are almost universally distributed into High Nucleic Acid content (HNA) and Low Nucleic Acid content (LNA) bacterial cells (Gasol et al. 1999; Huete-Stauffer and Moran 2012). Phylogenetic analyses also indicate that HNA and LNA groups are distinct (Schattenhofer et al. 2011). Not all cells are active within the bacterial community especially in oligotrophic environments where resources are scarce, and several diverse survival strategies take place (Morita 1997). HNA bacteria are considered to be metabolically active members of a given community, highly dynamic, responsible for around 95% of total bacterial carbon production and are significant in biogeochemical processes in the various aquatic ecosystems (Lebaron et al. 2001; Servais et al. 2003), while the cell-specific activity (CSA) of LNA bacteria is low and thus are regarded as inactive (Lebaron et al. 2001; 2002). These inactive or dormant cells can resume growth if placed in a nutrient-rich or favourable environment (Wang et al. 2009).

In this study, the bacterial production was also higher in the frontal regions. The production rate was approximately two to four fold higher in the frontal regions and showed a significant positive relation with HNA bacteria. This observation leads to a conclusion that HNA bacteria are more active than LNA and can be used as a proxy for measuring the active cells. A study by Longnecker et al. (2006) off the Oregon coast also observed high cell specific leucine and thymidine incorporation rates in HNA bacteria. The HNA bacteria are known to incorporate leucine at a faster rate, increase in cell size, and contribute significantly to bacterial production in the aquatic environments (Morán et al. 2011). The TBC, HNA bacteria and BP were higher in the frontal regions during PWM. This points out that seasonal driven changes in nutrient concentrations influence and regulates the bacterial populations in NEAS region.

Nutrient injections in the frontal zones often support bacterial production via an increase in primary production by the larger size phytoplankton (Videau et al. 1994). A concurrent study carried out in the NEAS frontal region also reported the dominance of larger phytoplankton (Prymnesiophytes) as well as high auto and heterotrophic activity (Roy et al. 2015; Sarma et al. 2015). Likewise, a few studies at the frontal regions of Northern Pacific subtropical gyres and California Current Ecosystem fronts also revealed the presence of larger phytoplankton cells (Diatoms and Prymnesiophytes), elevated primary and bacterial production in the fronts (Leonard et al. 2001; Juranek et al. 2012; Landry et al. 2012). In the present study, high HNA bacterial abundance and BP in the frontal regions of NEAS with high chlorophyll and nutrients indicate the

importance of organic matter released by phytoplankton as quality substrates for the sustenance of their population.

The DOM released by the algal cells has long been recognized as high quality substrates for bacteria (Cole et al. 1982). The factors such as dissolved organic matter and temperature tend to limit the bacterial growth rates (Kirchman et al. 1993). Moreover, the temperature has a greater effect on bacterial growth when compared to substrate supply (Yokokawa and Nagata 2005; Longnecker et al. 2006). A few studies have reported that an increase in bacterial abundance, growth rate, and phytoplankton biomass was related to nutrients which are also temperature dependent (Behrenfeld et al. 2006; Boyce et al. 2010). The observations under the Ocean Finder program identified the frontal regions by observing changes in the salinity and SST; the details are presented elsewhere (Vipin et al. 2015). During EWM, two relatively cold parcels of water were evident from the CTD data between 19.25–19.48 °N and 19.95–20.20 °N; in both the cases, the temperature decrease was 0.5–1.0 °C (Vipin et al. 2015). In the case of PWM, the difference in SST between fronts and non-fronts was about 0.56 to 1.02 °C (Sarma et al. 2015). However, this subtle change in temperature may not be significant in influencing the bacterial growth as observed in the temperate oceans, where the cross-frontal differences in SST and sea-surface salinity (SSS) are as large as 10-15 °C and 2-3 psu respectively (Belkin et al. 2009).

In the present study area, warm patch region showed a high abundance of LNA bacteria irrespective of the seasons. A possible reason for this could be that LNA bacteria are less dependent on phytoplankton substrates (Scharek and Latasa 2007) as most of the population includes dead or dormant cells. Increase in the chl *a* signature in the filament region showed availability of the nutrients for micro heterotrophs which resulted in the decrease of metabolically inactive LNA cells. A study by Belzile et al. (2008) observed a quick response of HNA over LNA cells during phytoplankton biomass accumulation event in Beaufort Shelf waters.

The present study indicated a significant increase in TEP, TBC, and BP from EWM to PWM. A significant negative correlation between TBC and TEP in the filament, as well as the frontal regions, indicate a possible role of bacteria in the fast turnover of the organic matter present in the frontal zones during both the seasons. Besides, an increase in HNA bacteria led to depletion of TEP possibly indicating their active utilization. Aggregate associated bacteria may contribute a significant fraction of bacterial production and remineralization in surrounding water column (Kiørboe and Jackson 2001). They solubilize particulate organic matter by expression of various enzymes depending on the substrate availability (Hollibaugh and Azam 1983). A study by Arnous et al. (2010) reported that

TEP is involved in the dynamics of bacteria and protozoa abundance in freshwater pelagic environments. Understanding the mechanisms involved in the expression of enzymes that are involved in the dissolution of TEP would be a step ahead.

Earlier studies have reported the distribution and influence of TEP on bacterial activity and their role in the biogeochemical process in the marine environment (Passow and Alldredge, 1994; Dam and Drapeau, 1995). A study by Ramaiah et al. (2000) during the summer monsoon in this region also suggested that bacterial metabolism is supported by the availability of the TEP in the Arabian Sea. In the present study, positive relation between TEP and Chl *a* in the front indicate the role of in situ production in generating TEP.

In this study, a low-saline surface patch was seen in the EWM-CTD section around 19.55 °N where no corresponding signatures of temperature and chlorophyll were observed. Interestingly, in this region signatures of TEP and HNA bacteria were seen. Vipin et al. (2015) suggested that this could be due to the rainfall event at (69.90 °E, 16.50 °N) and was related to advection. Long-distance advection of low-salinity patches is reported earlier from the central part of the Indian west coast (Shankar et al. 2005). The present study supports this hypothesis as the abundance of bacteria especially HNA bacteria and TEP were high, and the coastal production which is mainly dominated by bacteria during the rainfall might have advected with the water parcel. It is also possible that the presence of this biological signature could be due to the fronts that crossed this transect in the region earlier and could be a signature of a trailing front.

The standing stock of bacteria was similar up to 100 m depth in both frontal and non-frontal zones. Ducklow (1999) also pointed out, while explaining the pattern in the bacterial variability, that the bacterial standing stocks are similar in the euphotic zones ranging 35-135 m deep throughout the world ocean, while production rates vary more widely. This can be attributed to the differences in the metabolic activity of bacterial population as evident in this study. Sarma et al. (2015) suggested that physical mixing determines the conditions for a biological response to occur and is dependent on the age of the front. Roy and Anil (2015) pointed out that the convective mixing during the winter and ventilation of the subsurface water together with irradiance exerts ecological pressure on different phytoplankton enforcing changes in food web dynamics. Their observations also pointed out that low-light adapted *Prochlorococcus* population collapses during this period of intensive convective mixing and have significant implications possibly influencing the microbial loop. Studies elucidating the role of the microbial loop on food web dynamics and quantifying their influence on carbon export is a step ahead.

In pelagic ecosystems, predaceous protists are ubiquitous and range in size from 2  $\mu\text{m}$  flagellates to >100  $\mu\text{m}$  ciliates and dinoflagellates (Sherr and Sherr 2002). Sherr and Sherr (2002) also stated that predation by protists is a significant source of mortality for both autotrophic as well as heterotrophic bacteria. A significant positive correlation between protists and HNA bacteria was observed in the front during EWM. A previous study by Krstulović et al. (1998) also reported a strong positive relationship between bacteria and protists. In general, the standing stocks of aquatic bacterial communities are governed by two major factors, i.e., resource supply (both inorganic and organic nutrients), and predation (either by bacterivores or viral mortality) (Sherr and Sherr 2002). In the case of predation, bacterial cell size has a vital role in determining bacterial susceptibility to predation pressure (Gude 1989; Hahn and Hofle 2001). It has been reported that size-selective grazing by protists (mainly bacterivorous nanoflagellates (HNF)) exerts strong grazing pressure on medium and larger size cells (Lampert 1987; Montagnes et al., 2008). This could be one of the reasons for the preference of protists for HNA bacteria, as their size is larger than LNA bacteria. Other than cell size, taxonomic composition, cell morphology, and activity also have a pronounced role in predator-prey interactions (Gasol et al., 1999; Gasol and del Giorgio 2000; Gerea et al., 2013).

Overall, the present study indicated that the temporal variation in the abundance of bacteria and their activity in frontal regions was influenced by the early and peak winter monsoon conditions. Sarma et al. (2018) pointed out that the plankton response depended on the age of the front, and, more importantly, the initial or background conditions under which a front form. Further, their data also showed that the advection of fronts adds to this intraseasonal variability in the background condition which in turn influences the average concentration of nutrients or of biomass. In such a scenario, the response at each of the trophic levels would have a specific lag period which in itself is complex. The bacterial population will thus be influenced by trophic interactions. However, information regarding such short lived interactions in the tropical frontal system is non-existent except for the observations made herein and needs further attention.

### **Acknowledgments**

The authors would like to thank The Director, NIO, for his support and the captain, officers and crew members of SSK # 041 and SSK # 060 cruise for helping us on-board. We are thankful to Dr. D Shankar and Dr. S.G. Aparna for the helpful discussion. We also thank other members of the cruise

Formatted: Indent: First line: 0.32", Space After: 6 pt, Line spacing: 1.5 lines

Formatted: Space After: 6 pt, Line spacing: 1.5 lines

and Ocean Finder team mates. The present study was supported by the OCEAN FINDER programme PSC 0105 of CSIR-NIO. This is NIO contribution XXXX

## References

- Arnous MB, Courcol N, Carrias JF (2010) The significance of transparent exopolymeric particles in the vertical distribution of bacteria and heterotrophic nanoflagellates in Lake Pavin. *Aquat Sci* 72:245–253.
- Azam F, Fenchel T, Field JG, Gray JS, Meyer-Reil LA, Thingstad F (1983) The ecological role of water-column microbes in the sea. *Mar Ecol Prog Ser* Oldendorf. 10:257-263.
- Banse K, McClain CR (1986) Satellite-observed winter blooms of phytoplankton in the Arabian Sea. *Mar Ecol Prog Ser* 34:201-211.
- Behrenfeld MJ, O'Malley RT, Siegel DA, McClain CR, Sarmiento JL, Feldman GC, Milligan AJ, Falkowski PG, Letelier RM, Boss ES (2006) Climate-driven trends in contemporary ocean productivity. *Nature* 444:752-755.
- Belkin IM, Cornillon PC, Sherman K (2009) Fronts in large marine ecosystems. *Prog Oceanogr* 81:223–236.
- Belzile C, Brugel S, Nozais C, Gratton Y, Demers S (2008) Variations of the abundance and nucleic acid content of heterotrophic bacteria in Beaufort Shelf waters during winter and spring. *J Mar Syst* 74:946-956.
- Boyce DG, Lewis MR, Worm B (2010) Global phytoplankton decline over the past century. *Nature* 466:591-596.
- Chin-Leo G, Benner R (1992) Enhanced bacterioplankton production and respiration at intermediate salinities in the Mississippi River plume. *Mar Ecol Prog Ser* 87:87.
- Christaki U, Courties C, Massana R, Catala P, Lebaron P, Gasol JM, Zubkov MV (2011) Optimized routine flow cytometric enumeration of heterotrophic flagellates using SYBR Green I. *Limnol Oceanogr Methods* 9:329-339.
- Cole JJ, Likens GE, Strayer DL (1982) Photosynthetically produced dissolved organic carbon: An important carbon source for planktonic bacteria. *Limnol Oceanogr* 27:1080-1090.
- Dam HG, Drapeau DT (1995) Coagulation efficiency, organic matter glues and the dynamics of particles during a phytoplankton bloom in a mesocosm study. *Deep-Sea Res II* 42:111–124.
- Ducklow HW (1993) Bacterioplankton distributions and production in the north western Indian Ocean and Gulf of Oman, September 1986. *Deep-Sea Res II* 40:753-771.
- Ducklow HW (1999) The bacterial component of the oceanic euphotic zone. *FEMS Microbiol Ecol* 30:1-10.
- Eswaran R, Khandeparker L (2017) Seasonal variation in bacterial community composition and  $\beta$ -glucosidase expression in a tropical monsoon-influenced estuary. *Aquat Microb Ecol* 80:273-287.
- Fernández M, Bianchi M, Van Wambeke F (1994) Bacterial biomass, heterotrophic production and utilization of dissolved organic matter photosynthetically produced in the Almeria-Oran front. *J*

Mar Syst 5:313-325.

- Gasol JM, Zweifel UL, Peters F, Fuhrman JA, Hagström A (1999) Significance of size and nucleic acid content heterogeneity as measured by flow cytometry in natural planktonic bacteria. *Appl Environ Microbiol* 65:4475-4483.
- Gasol JM, Del Giorgio PA (2000) Using flow cytometry for counting natural planktonic bacteria and understanding the structure of planktonic bacterial communities. *Sci Mar* 64:197-224.
- Garrison DL, Gowing MM, Hughes MP, Campbell L, Caron DA, Dennett MR, Shalapyonok A, Olson RJ, Landry MR, Brown SL, Liu HB (2000) Microbial food web structure in the Arabian Sea: a US JGOFS study. *Deep Sea Res Part II: Top Stud Oceanogr* 47:1387-1422.
- Gerea M, Queimalinos C, Schiaffino MR, Izaguirre I, Forn I, Massana R, Unrein F (2013) In situ prey selection of mixotrophic and heterotrophic flagellates in Antarctic oligotrophic lakes: an analysis of the digestive vacuole content. *J Plankton Res* 35:201-212.
- Grossart HP, Simon M (1997) Formation of macroscopic organic aggregates (lake snow) in a large lake: the significance of transparent exopolymer particles, phytoplankton, and zooplankton. *Limnol Oceanogr* 42:1651-1659.
- Grossart HP, Czub G, Simon M (2006) Algae-bacteria interactions and their effects on aggregation and organic matter flux in the sea. *Environ Microbiol* 8:1074-1084.
- Gude H (1989) The role of grazing on bacteria in plankton succession. In U Sommer (ed.), *Plankton ecology. Succession in plankton communities*. Springer Verlag, Berlin, Germany 337-364.
- Hahn MW, Hofle MG (2001) Grazing of protozoa and its effect on populations of aquatic bacteria. *FEMS Microbiol Ecol* 35:113-121.
- Hamasaki K, Long RA, Azam F (2004) Individual cell growth rates of marine bacteria, measured by bromodeoxyuridine incorporation. *Aquat Microb Ecol* 35:217-227.
- Hollibaugh JT, Azam F (1983) Microbial-degradation of dissolved proteins in seawater. *Limnol Oceanogr* 28:1104-1116.
- Huete-Stauffer TM, Morán XAG (2012) Dynamics of heterotrophic bacteria in temperate coastal waters: similar net growth but different controls in low and high nucleic acid cells. *Aquat Microb Ecol* 67:211-223.
- Juranek LW, Quay PD, Feely RA, Lockwood D, Karl DM, Church MJ (2012) Biological production in the NE Pacific and its influence on air-sea CO<sub>2</sub> flux: Evidence from dissolved oxygen isotopes and O<sub>2</sub>/Ar. *J Geophys Res Oceans* 117.
- Khandeparker L, Eswaran R, Gardade L, Kuchi N, Mapari K, Naik SD, Anil AC (2017) Elucidation of the tidal influence on bacterial populations in a monsoon influenced estuary through simultaneous observations. *Environ Monit Assess* 189:41.
- Klein C, Claquin P, Pannard A, Napoléon C, Le Roy B, Véron B (2011) Dynamics of soluble extracellular polymeric substances and transparent exopolymer particle pools in coastal ecosystems. *Mar Ecol Prog Ser* 427:13-27.

- Kiørboe T, Jackson GA (2001) Marine snow, organic solute plumes, and optimal chemosensory behavior of bacteria. *Limnol Oceanogr* 46:1309-1318.
- Kirchman DL, Keil RG, Simon M, Welshmeyer NA (1993) Biomass and production of heterotrophic bacterioplankton in the oceanic subarctic Pacific. *Deep-Sea Res* 40:967– 988.
- Krstulović N, Šolić M, Marasović I (1998) Relationship between bacteria, phytoplankton and heterotrophic nanoflagellates along the trophic gradient. *Helgoland Mar Res* 51:433-443.
- Lampert W (1987) Predictability in lake ecosystems: the role of biotic interactions, *In* ED Schulze and H Zwölfer (ed.), *Potential and limitations of ecosystem analysis. Ecological studies*, Springer-Verlag, Berlin, Germany 61:333-346.
- Landry MR, Ohman MD, Goericke R, Stukel MR, Barbeau KA, Bundy R, Kahru M (2012) Pelagic community responses to a deep-water front in the California Current Ecosystem: overview of the A-Front Study. *J Plankton Res* 025.
- Lebaron P, Servais P, Agogue H, Courties C, Joux F (2001) Does the high nucleic acid content of individual bacterial cells allow us to discriminate between active cells and inactive cells in aquatic systems? *Appl Environ Microbiol* 67:1775–1782.
- Lebaron P, Servais P, Baudoux AC, Bourrain M, Courties C, Parthuisot N (2002) Variations of bacterial-specific activity with cell size and nucleic acid content assessed by flow cytometry. *Aquat Microb Ecol* 28:131–140.
- Leonard CL, Bidigare RR, Seki MP, Polovina JJ (2001) Interannual mesoscale physical and biological variability in the North Pacific Central Gyre. *Prog Oceanogr* 49:227-244.
- Lohmann R, Belkin IM (2014) Organic pollutants and ocean fronts across the Atlantic Ocean: A review. *Prog Oceanogr* 128:172 – 184.
- Longnecker K, Sherr BF, Sherr EB (2006) Variation in cell-specific rates of leucine and thymidine incorporation by marine bacteria with high and with low nucleic acid content off the Oregon coast. *Aquat Microb Ecol* 43:113–25
- Madhupratap M, Prasanna Kumar S, Bhattathiri PMA, Dileep Kumar M, Raghukumar S, Nair KKC, Ramaiah N (1996) Mechanism of the biological response to winter cooling in the northeastern Arabian Sea. *Nature*. 384:549–552.
- Montagnes DJS, Barbosa AB, Boenigk J, Davidson K, Jürgens K, Macek M, Parry, J.D., Roberts EC, Šimek K (2008) Selective feeding behaviour of key free-living protists: avenues for continued study. *Aquat Microb Ecol* 53:83–98.
- Morán XAG, Ducklow HW, Erickson M (2011) Single-cell physiological structure and growth rates of heterotrophic bacteria in a temperate estuary (Waquoit Bay, Massachusetts). *Limnol Oceanogr* 56:37–48.
- Morita RY 1997. *Bacteria in oligotrophic environments*. Chapman and Hall, New York.
- Muelbert JH, Acha M, Mianzan H, Guerrero R, Reta R, Braga ES, Garcia VMT, Barasategui A, Gomez-Erache M, Ramirez F (2008) Biological, physical and chemical properties at the

subtropical shelf front zone in the SW Atlantic continental shelf. *Cont Shelf Res* 28:1662-1673.

Nelson CE, Carlson CA (2005) A non-radioactive assay of bacterial productivity optimized for oligotrophic pelagic environments. *Limnol Oceanogr* 50:211-220.

Passow U, Alldredge AL (1994) Distribution, size and bacterial colonization of transparent exopolymeric particles (TEP) in the ocean. *Mar Ecol Prog Ser* 113:185-198.

Passow U (2002) Transparent exopolymer particles (TEP) in aquatic environments. *Prog Oceanogr* 55:287-333.

Pedros-Alíó C, Calderó-Paz JI, Guixa-Boixereu N, Estrada M, Gasol JM (1999) Bacterioplankton and phytoplankton biomass and production during summer stratification in the north western Mediterranean Sea. *Deep-Sea Res I* 46:985-1019.

Pernthaler A, Pernthaler J, Schattner M, Amann R (2002) Identification of DNA-synthesizing bacterial cells in coastal North Sea plankton. *Appl Environ Microbiol* 68 :728-5736.

Pomeroy A, Joint I (1999) Bacterioplankton activity in the surface waters of the Arabian Sea during and after the 1994 SW monsoon. *Deep-Sea Res II* 46:767-794.

Ramaiah N, Raghukumar S, Gauns M (1996) Bacterial abundance and production in the central and eastern Arabian Sea. *Curr Sci* 71:878-882.

Ramaiah N, Sarma VVSS, Gauns M, Kumar MD, Madhupratap M (2000) Abundance and relationship of bacteria with transparent exopolymer particles during the 1996 summer monsoon in the Arabian Sea; *Proc. Indian Academy of Sciences (Earth Planet. Sci.)* 109: 1-9.

Read JF, Lucas MI, Holley SE, Pollard RT (2000) Phytoplankton, nutrients and hydrography in the frontal zone between the Southwest Indian Subtropical gyre and the Southern Ocean. *Deep-Sea Res I* 47:2341-2367.

Roy R, Anil AC (2015) Complex interplay of physical forcing and *Prochlorococcus* population in ocean. *Prog Oceanogr* 137:250-260.

Roy R, Chitari R, Kulkarni V, Krishna MS, Sarma VVSS, Anil AC (2015) CHEMTAX-derived phytoplankton community structure associated with temperature fronts in the northeastern Arabian Sea. *J Mar Syst* 144:81-91.

Samo TJ, Pedler BE, Ball GI, Pasulka AL, Taylor AG, Aluwihare LI, Azam F, Ralf G, Landry MR (2012) Microbial distribution and activity across a water mass frontal zone in the California Current Ecosystem. *J Plankton Res* 34:802-814.

Sanders R, Henson SA, Koski M, De La Rocha CL, Painter SC, Poulton AJ, Riley J, Salihoglu B, Visser A, Yool A, Bellerby R, Martin AP (2014) The Biological Carbon Pump in the North Atlantic. *Prog Oceanogr* 129:200-218.

Sarma VVSS, Delabehra HB, Sudharani P, Remya R, Patil JS, Desai DV (2015) Variations in the inorganic carbon components in the thermal fronts during winter in the northeastern Arabian Sea. *Mar Chem* 169:16-22.

- Sarma VVSS, Desai DV, Patil JS, Khandeparker L, Aparna SG, Shankar D, D'Souza S, Dalabehera HB, Mukherjee J, Sudharani P, Anil AC (2018) Ecosystem response in temperature fronts in the northeastern Arabian Sea. *Prog Oceanogr* <https://doi.org/10.1016/j.pocean.2018.02.004>.
- Scharek R, Latasa M (2007) Growth, grazing and carbon flux of high and low nucleic acid bacteria differ in surface and deep chlorophyll maximum layers in the NW Mediterranean Sea. *Aquat Microb Ecol* 46:153-161.
- Schattenhofer M, Wulf J, Kostadinov I, Glöckner OF, Zubkov MV, Fuchs BM (2011) Phylogenetic characterisation of picoplanktonic populations with high and low nucleic acid content in the North Atlantic Ocean. *Syst Appl Microbiol* 34:470-475.
- Schuster S, Herndl GJ (1995) Formation and significance of transparent exopolymer particles in the northern Adriatic Sea. *Mar Ecol Prog Ser* 124:227-236.
- Servais P, Casamayor EO, Courties C, Catala P, Parthuisot N, Lebaron P (2003) Activity and diversity of bacterial cells with high and low nucleic acid content. *Aquat Microb Ecol* 33:41-51.
- Shankar D, Shenoi SSC, Nayak RK, Vinayachandran PN, Nampoothiri G, Almeida AM, Michael GS, Ramesh Kumar MR, Sundar D, Sreejith OP (2005) Hydrography of the eastern Arabian Sea during summer monsoon 2002. *J Earth Syst Sci* 114:459-474.
- Sherr EB, Sherr BF (2002) Significance of predation by protists in aquatic microbial food webs. *A Van Leeuw* 81:293-308.
- Solanki HU, Mankodi PC, Dwivedi RM, Nayak SR (2008) Satellite observations of main oceanographic processes to identify ecological associations in the Northern Arabian Sea for fishery resources exploration. *Hydrobiologia* 612:269-279.
- Søndergaard M, Williams PJ, Cauwet G, Riemann B, Robinson C, Terzic S, Woodward EM, Worm J (2000) Net accumulation and flux of dissolved organic carbon and dissolved organic nitrogen in marine plankton communities. *Limnol Oceanogr* 45:1097-111.
- Steward GF, Azam F (1999) Bromodeoxyuridine as an alternative to 3H-thymidine for measuring bacterial productivity in aquatic samples. *Aquat Microb Ecol* 19:57-66.
- Tarran GA, Zubkov MV, Sleigh MA, Burkill PH, Yallop M (2001) Microbial community structure and standing stocks in the NE Atlantic in June and July of 1996. *Deep-Sea Res II* 48:963-985.
- Taylor AG, Goericke R, Landry MR, Selph KE, Wick DA, Roadman MJ (2012) Sharp gradients in phytoplankton community structure across a frontal zone in the California Current Ecosystem. *J Plankton Res* 34:778-789.
- Vipin P, Kankan S, Aparna SG, Shankar D, Sarma VVSS, Gracias DG, Krishna MS, Srikanth G, Mandal R, Rama Rao EP, Srinivasa Rao N (2015) Evolution and sub-surface characteristics of a sea-surface temperature filament and front in the northeastern Arabian Sea during November-December 2012. *J Mar Syst* 150:1-11.
- Videau C, Sourmia A, Prieur L, Fiala M (1994) Phytoplankton and primary production characteristics at selected sites in the geostrophic Almeria-Oran front system (SW Mediterranean Sea). *J Mar*

Formatted: Space After: 12 pt, Line spacing: single

Syst 5:235-250.

- | Wang Y, Hammes F, Boon N, Chami M, Egli T (2009) Isolation and characterization of low nucleic acid (LNA)-content bacteria. *The ISME J* 3:889–902.
- | Wiebinga CJ, Veldhuis MJ, De Baar HJ (1997) Abundance and productivity of bacterioplankton in relation to seasonal upwelling in the northwest Indian Ocean. *Deep-Sea Res I* 44:451-476.
- | Yokokawa T, Nagata T (2005) Growth and grazing mortality rates of phylogenetic groups of bacterioplankton in coastal marine environments. *Appl Environ Microbiol* 71:6799 - 6807.

Formatted: Space After: 6 pt, Line spacing: single

Formatted: Justified, Line spacing: single

Formatted: Space After: 12 pt, Line spacing: single

### Legends to Figures:

**Fig. 1.** Map showing sampling stations (EWM and PWM cruise – Ocean Finder programme) in the north-eastern Arabian Sea (NEAS).

**Fig. 2. a)** Satellite sea surface temperature (SST; temperature) image illustrating the formation of filament (denoted by red curve) and front (denoted by pink curve). **b)** Vertical profiles of temperature ( $^{\circ}\text{C}$ , first panel), salinity (second panel) and chlorophyll *a* ( $\text{mg m}^{-3}$ , third panel) measured during the EWM CTD transect. The sampling locations are marked by inverted triangles on the top axis of the temperature panel in the warm patch region, the black asterisks designate stations in the filament and the circle designates stations in the frontal region. The dashed lines in these three panels denote the base of the mixed layer.

**Fig. 3. a)** Satellite SST image illustrating the formation of fronts (denoted by red and blue line), **b)** Vertical profiles of temperature ( $^{\circ}\text{C}$ , first panel), salinity (second panel) and chlorophyll *a* ( $\text{mg m}^{-3}$ , third panel) measured during the PWM CTD transects (T1 and T2). The sampling locations are marked by inverted triangles on the top axis of the temperature panel in the non-frontal region, the black asterisks designate stations in the frontal region. The dashed lines in these three panels denote the base of the mixed layer.

**Fig. 4.** Spatial and vertical profiles of **a)** Total Bacterial Count (TBC), **b)** High nucleic acid content (HNA) bacteria, **c)** Low nucleic acid content (LNA) bacteria, **d)** Protists abundance, **e)** the ratio of bacteria: protists, and **f)** Transparent exopolysaccharides (TEP). Cell abundance expressed as cells  $\text{L}^{-1}$  during EWM cruise. Dots indicate the sampled depth and dotted line indicates the variability in the mixed layer depth along the section.

**Fig. 5.** Depth integrated values of **a)** total bacterial count (TBC), High nucleic acid (HNA) bacteria and Low nucleic acid (LNA) bacteria, **b)** Protist abundance, **c)** Transparent exopolysaccharides (TEP) and Chlorophyll *a* (Chl *a*) concentration during the EWM cruise.

**Fig. 6.** Spatial and vertical profiles of **a)** Total Bacterial Count (TBC), **b)** Bacterial production (BP), **c)** High nucleic acid content (HNA) bacteria, **d)** Protists, **e)** Low nucleic acid content (LNA) bacteria, **f)** Bacteria: Protists ratio and **g)** transparent exopolysaccharides (TEP) during PWM cruise. Cell abundance is expressed as cells  $\text{L}^{-1}$ . Dots indicate the sampled depth and dotted line indicates the variability in the mixed layer depth along the section.

**Fig. 7.** Depth integrated values of **a)** total bacterial count (TBC), High nucleic acid (HNA) bacteria and Low nucleic acid (LNA) bacteria, **b)** Protist abundance, **c)** Transparent exopolysaccharides (TEP) and Chlorophyll *a* (Chl *a*) concentration during the PWM cruise.

### Legends to Tables:

Table 1: Results of correlation analyses ('r', between (a) biotic ((HNA & LNA) bacteria, chlorophyll *a*, protists and TEPs, and (b) abiotic variables (Bonferroni corrected with significance at  $p \leq 0.01$ ) during EWM.

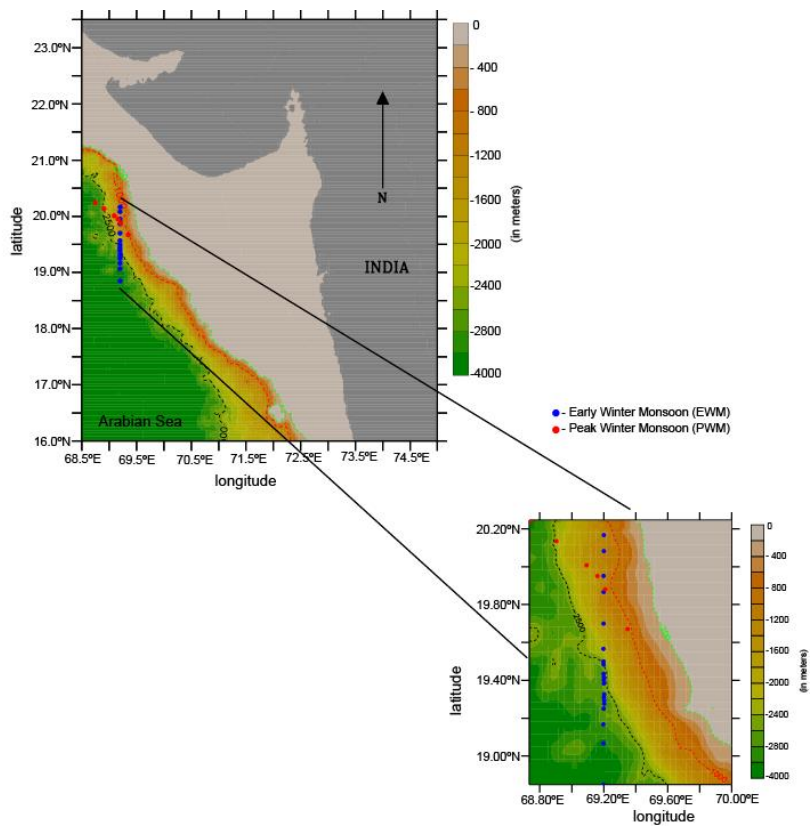


Fig. 1

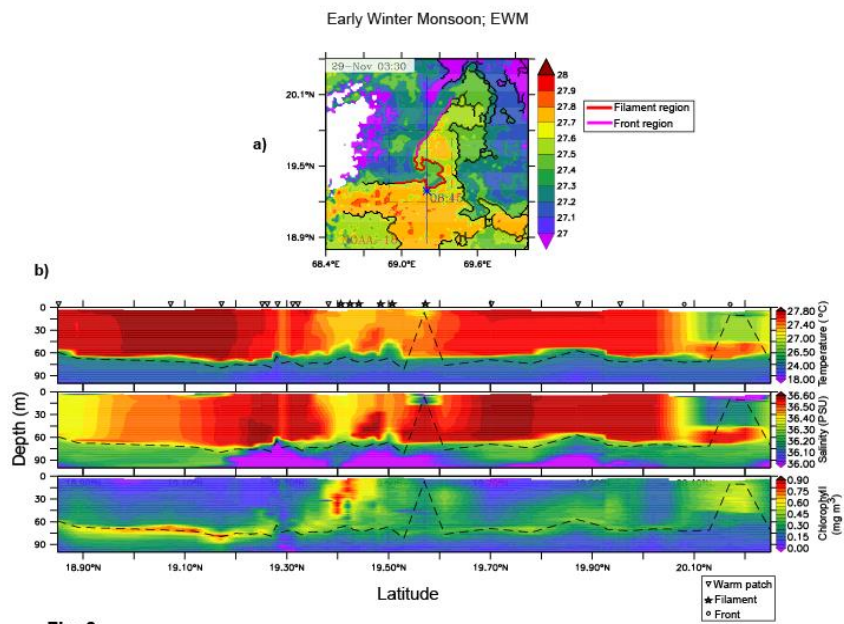


Fig. 2

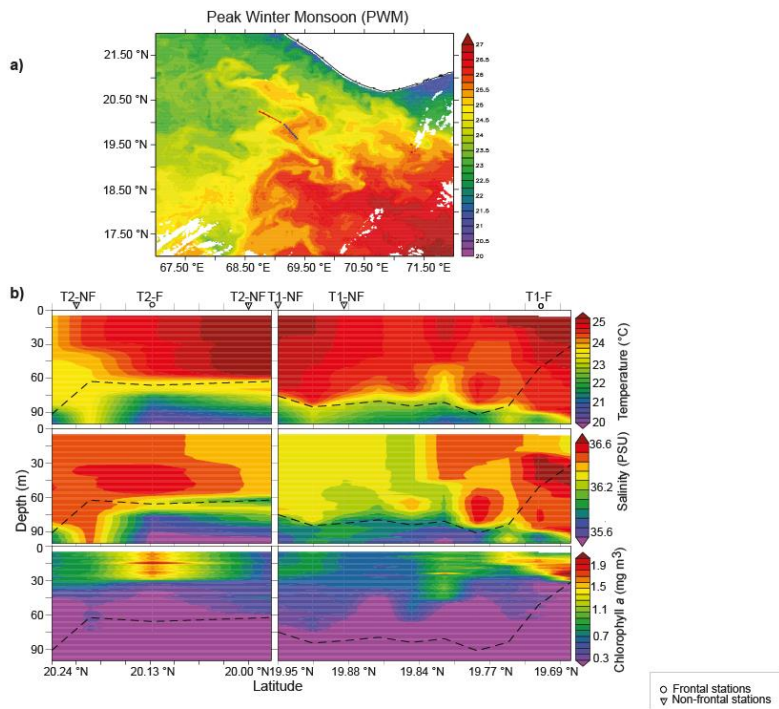


Fig. 3

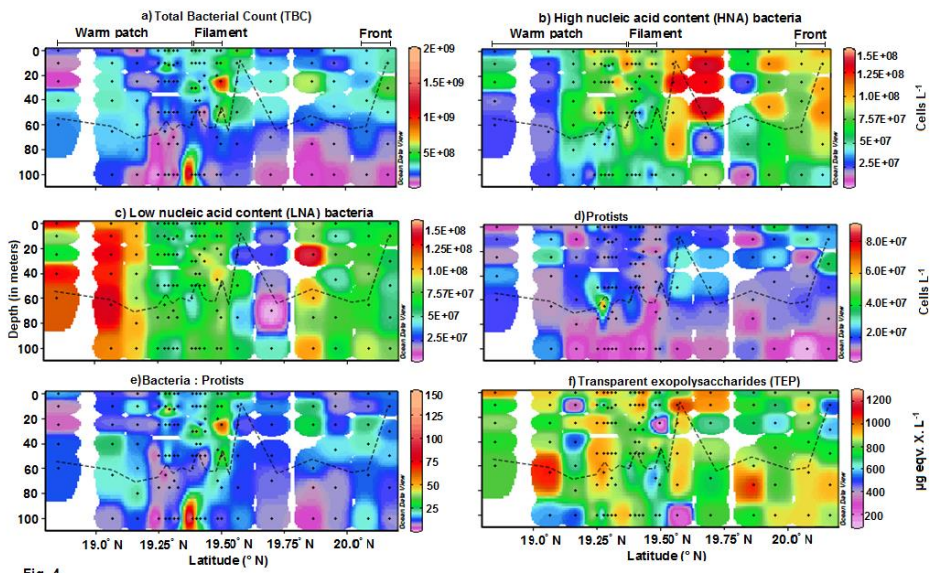


Fig. 4

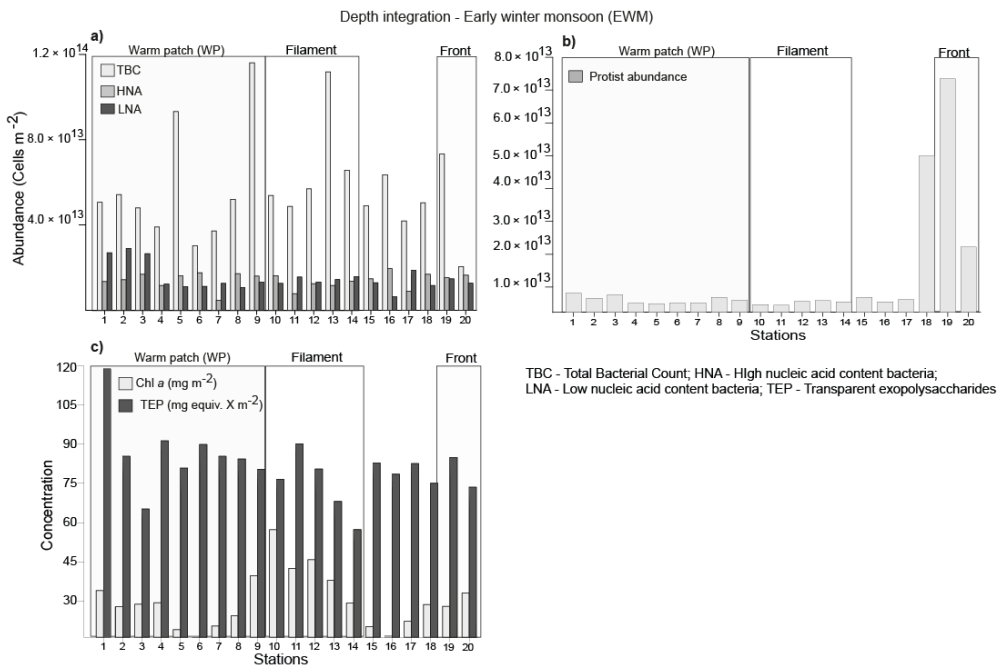


Fig. 5

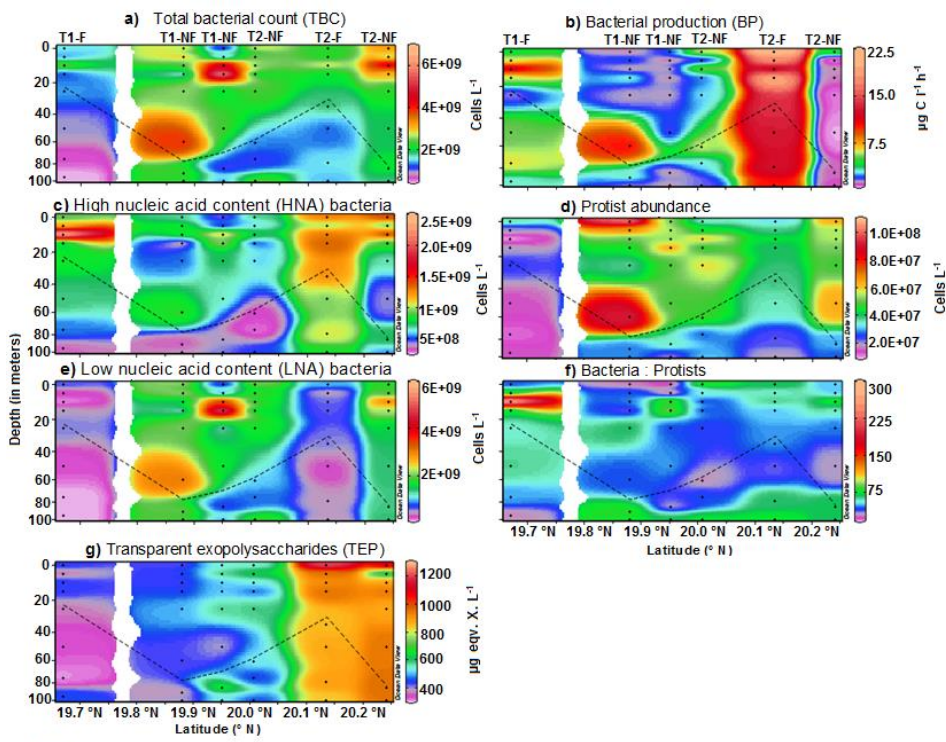


Fig. 6

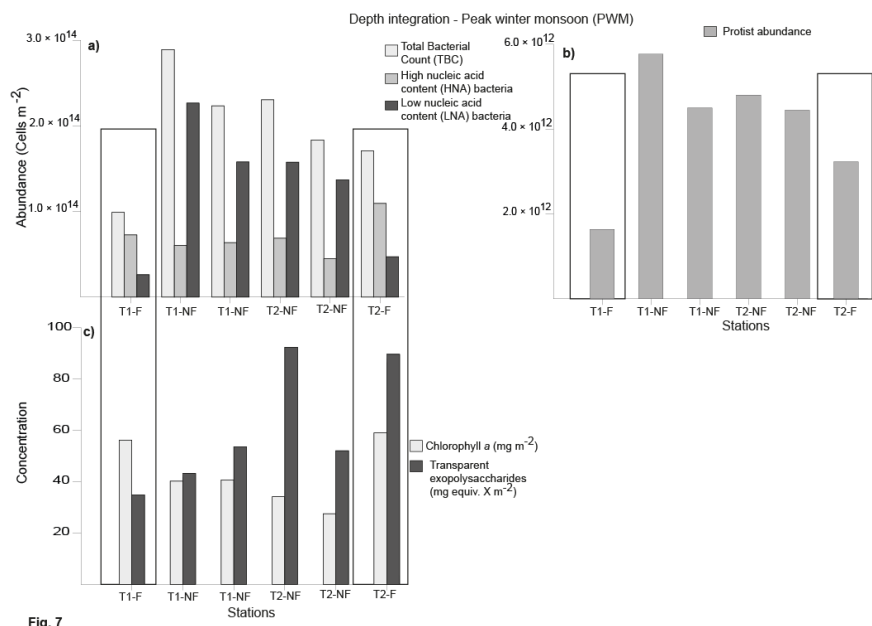


Fig. 7

Table 1: Results of correlation analyses ('r', between (a) biotic (HNA & LNA) bacteria, chlorophyll  $\alpha$ , protists and TEPs, and (b) abiotic variables (Bonferroni corrected with significance at  $p \leq 0.01$ ) during EWM.

(a) Biotic variables

S.No	Parameters	Warm patch (N = 55)		Filament (N = 30)		Front (N = 12)		
		r	P ( $\leq 0.01$ )	r	P ( $\leq 0.01$ )	r	P ( $\leq 0.01$ )	
1	TBC vs	TEP	0.14	0.31	- 0.50	0.005	- 0.70	0.01
		HNA	0.22	0.12	0.48	0.007	0.75	0.004
		LNA	0.06	0.68	0.08	0.69	- 0.45	0.14
		Protists	- 0.05	0.71	0.29	0.11	0.84	0.001
2	Protists vs	HNA	0.01	0.96	0.42	0.02	0.70	0.01
		LNA	- 0.00	0.96	- 0.14	0.44	- 0.55	0.06
		TEP's	0.08	0.52	0.02	0.89	- 0.51	0.08
3	Chl $\alpha$ vs	TBC	- 0.03	0.18	0.17	0.41	0.94	0.000
		Protists	0.10	0.44	0.12	0.30	0.81	0.002
		HNA	- 0.01	0.92	0.38	0.07	0.76	0.004
		TEP	0.07	0.58	0.31	0.09	- 0.66	0.019
4.	TEP vs	HNA	0.05	0.67	-0.07	0.72	-0.38	0.22
		LNA	-0.06	0.62	0.02	0.90	0.11	0.72
		Protists	0.08	0.53	0.02	0.89	-0.51	0.09
		Chl $\alpha$	0.07	0.58	0.31	0.09	-0.66	0.02

TBC – Total Bacterial Count; TEP – Transparent Exopolysaccharides; HNA – High nucleic acid content cells; LNA – Low nucleic acid content cells; Chl  $\alpha$  – Chlorophyll  $\alpha$

b) Abiotic variables

S. No	Parameters	Warm patch (N = 55)		Filament (N = 30)		Front (N = 12)		
		r	P ( $\leq 0.01$ )	r	P ( $\leq 0.01$ )	r	P ( $\leq 0.01$ )	
1.	Temperature vs	TBC	-0.00	0.96	<b>0.43</b>	<b>0.01</b>	<b>0.77</b>	<b>0.003</b>
		HNA	0.22	0.11	<b>0.47</b>	<b>0.01</b>	<b>0.76</b>	<b>0.004</b>
		LNA	0.08	0.55	-0.00	0.96	-0.45	0.14
		Protists	0.33	0.01	0.37	0.04	0.59	0.03
		Chl $\alpha$	0.03	0.80	<b>0.72</b>	<b>0.000</b>	<b>0.75</b>	<b>0.005</b>
2.	Nitrate vs	TBC	0.094	0.51	-0.38	0.03	<b>-0.72</b>	<b>0.008</b>
		HNA	-0.20	0.16	-0.32	0.07	<b>-0.80</b>	<b>0.002</b>
		LNA	-0.07	0.50	-0.06	0.75	0.66	0.02
		Protists	-0.35	0.01	-0.27	0.14	-0.69	0.12
		Chl $\alpha$	0.10	0.47	<b>-0.56</b>	<b>0.001</b>	<b>-0.73</b>	<b>0.007</b>
3.	Phosphate vs	TBC	0.21	0.12	-0.13	0.47	<b>-0.70</b>	<b>0.01</b>
		HNA	-0.15	0.30	<b>-0.46</b>	<b>0.009</b>	<b>-0.77</b>	<b>0.003</b>
		LNA	-0.01	0.90	0.04	0.81	0.63	0.02
		Protists	-0.23	0.10	-0.32	0.08	-0.63	0.02
		Chl $\alpha$	0.15	0.26	<b>-0.53</b>	<b>0.003</b>	<b>-0.69</b>	<b>0.01</b>
4.	Silicate vs	TBC	-0.09	0.48	-0.32	0.09	<b>-0.73</b>	<b>0.006</b>
		HNA	-0.30	0.03	-0.20	0.32	<b>-0.70</b>	<b>0.01</b>
		LNA	-0.00	0.96	-0.28	0.12	0.46	0.13
		Protists	-0.23	0.09	-0.34	0.06	<b>-0.66</b>	<b>0.01</b>
		Chl $\alpha$	0.00	0.96	-0.42	0.02	<b>-0.72</b>	<b>0.007</b>
5.	Nitrite vs	TBC	0.03	0.78	-0.26	0.16	-0.16	0.61
		HNA	-0.22	0.11	<b>-0.47</b>	<b>0.009</b>	0.06	0.84
		LNA	0.25	0.06	0.03	0.83	-0.02	0.95
		Protists	0.12	0.37	-0.23	0.23	-0.17	0.59
		Chl $\alpha$	0.07	0.57	-0.26	0.15	-0.05	0.85

TBC – Total Bacterial Count; HNA – High nucleic acid content cells; LNA – Low nucleic acid content cells; Chl  $\alpha$  – Chlorophyll  $\alpha$

